Simulation of Semiconductor Processes and Devices 2016
Edited by E. Bär, J. Lorenz, and P. Pichler

3D simulation of light exposure and resist effects in laser direct write lithography

Temitope Onanuga and Andreas Erdmann
Fraunhofer Institute for Integrated Systems and Device Technology, Schottkystrasse 10, 91058 Erlangen, Germany
Friedrich-Alexander-Universität Erlangen-Nürnberg, Graduate School of Advanced Optical Technologies SAOT,
Paul Gordan Strasse 6, 91052 Erlangen, Germany
Friedrich-Alexander-Universität Erlangen-Nürnberg, Chair of Electron Devices, Cauerstrasse 6, 91058 Erlangen, Germany

***Abstract*—We present a simulation approach that includes light and photoresist effects in laser direct write lithography (LDWL). This simulation flow allows to predict how the fabricated structure changes with variation in the process parameters. Using this simulation approach, we compute the change in feature size or critical dimension (CD) versus laser power and writing speed. The obtained simulation result agrees with experimental results. We extend this simulation method to predict the axial resolution of woodpile like structures and mesa arrays, which provide interesting patterns for metamaterials.**

I. Introduction

Laser Direct Write Lithography (LDWL) is a maskless patterning technique where a focused light beam is scanned over a light sensitive polymer (photo-resist) to generate desired patterns. The absence of photomasks in LDWL makes it cheaper and more flexible in comparison with projection lithography. However, LDWL is mostly based on serial writing, making it slower than projection lithography. In addition, the feature sizes and resolution of standard LDWL systems is in the order of $500nm$ [1]–[3], compared to $30nm$ for state of the art projection lithography systems.

The development of sub-wavelength projection lithography was accompanied and supported by the development and application of computational models. Such models describe optical and chemical effects during the exposure and processing of the photoresist. This paper proposes a corresponding model and simulation flow for LDWL.

Section II discusses the simulation flow in details. The application of the developed modeling approach for computing axial resolution is described in section III.

II. Model

The simulation flow is divided into four stages: bulk image, exposure, dark polymerization, and development. Figure 1 summarizes the effects covered in our model. This method can be applied for the standard single-photon absorption process (SPA) and multi-photon absorption processes. The models were implemented into our lithography simulator Dr. LiTHO [4], which is an established tool for the simulation of lithographic processes for the fabrication of semiconductor nanoelectronic devices.

A. Bulk Image

The bulk image is the 3D intensity distribution in the resist. This intensity distribution depends on the incident laser beam profile, numerical aperture (NA), and the refractive index and absorption of the immersion medium. The incident laser beam in most cases could be assumed to have a Gaussian profile.

We computed the bulk image using the paraxial approximation, Debye method [5] and Waveguide method [6]. The paraxial approximation is a scalar computation, based on the assumption of small angles between the propagating beam and the propagation axis. As the NA increases, the paraxial approximation differs more from the experimentally observed results. For example, for a typical NA of 1.4 and a x-polarized laser beam, the focused field is elongated in the x-direction compared to the y direction. Such effect is modeled by vectorial models. The Debye model [5] and waveguide computation [6] are vectorial models based on angular spectrum propagation of plane waves.

Table I presents the parameter values used in the computation of the bulk image.

B. Exposure

The photoresist material in LDWL typically contains a photosensitive material, monomer, and quenchers [8]. The photosensitive component of the resist absorbs light, gets excited, and decays to generate photo-radicals. Absorption reactions in the photoresist also lead to heat generation and increase in temperature of the focal regions. The extent of this local temperature change depends on the intensity, exposure duration, and material properties of the resist: heat capacity,

TABLE I: Laser and resist parameters

Parameter	*Value*	*Units*	*Reference*
laser power	5	mW	[2]
laser wavelength (λ)	0.78	μm	[7]
objective NA (NA)	1.0, 1.4	no units	[1]
immersion index	1.6	no units	[7]
resist thickness	20.	μm	choice
reflection co-efficient	0.001	no units	choice
linear absorption coefficient	$2. \times 10^{-4}$	cm^{-1}	choice
repetition rate	80	MHz	[1]
pulse duration	150	fs	[1]

978-1-5090-0818-6/16/$31.00 ©2016 IEEE

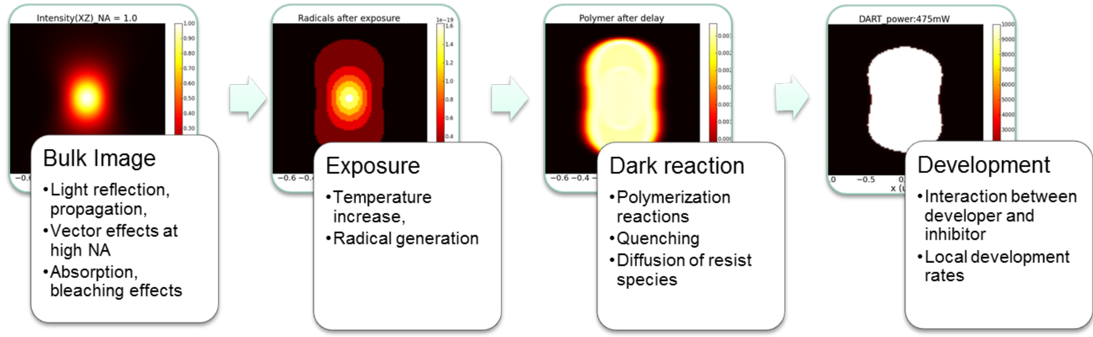

Fig. 1: Flowchart outlining the reactions considered at the different simulation levels: bulk image, exposure, dark reaction and development

density, and enthalpy of polymerization. In an Arrhenius-type model, the increase in temperature leads to an exponential increase in diffusion and reaction rates [9], [10]. The temperature rise of the focused region of the resist ranges from 0 to 10 degrees for a normal LDWL writing process [2].

The thermal effect is modeled using the well-known heat equation:

$$\frac{\partial T}{\partial t} = \frac{\kappa}{\rho c_p}\nabla^2 T + \frac{\alpha I[M]}{\rho c_p} + \frac{H}{\rho c_p}\frac{\partial [M]}{\partial t} \tag{1}$$

κ is the thermal conductivity of the resist, ρ is the density of the resist, c_p the specific heat capacity, α the molar absorption coefficient of the monomer, and ([M]) is the amount of monomers.

The amount of generated radicals is assumed to be equal to the amount of excited photosensitive material. For a two photon absorption (TPA) process [7]:

$$[R] = [Psc]_0 - [Psc]_0 \exp(-{n_{photons}}^2 \times 0.5 \times \delta_{TPA} \times t_{exp}) \tag{2}$$

Where $[R]$ is the amount of generated radicals, $[Psc]_0$ is the initial concentration of photosensitive material, δ_{SPA} and $\delta_{TPA}$are the SPA and TPA cross-sections and $n_{photons}$ is the photon flux corresponding to the absorbed intensity. t_{exp} is the exposure duration.

Table II shows the parameters used in simulating the exposure phase and the corresponding literature reference. The initial temperature was assumed to be 293K (about room temperature). The quantum yield of absorption was taken as a model fitting parameter so that the exposure duration and the laser powers in the simulations are close to the usual writing parameters in LDWL experiments. Typical experimental writing parameters are: laser power- $1-10mW$, exposure duration per spot- $0.01ms - 10ms$ [3], [1].

C. Dark Phase

Photoresist materials commonly used in LDWL include ORMOCER (Microresist Technologies, Germany) [11], SU-8 epoxy resin (developed by IBM) [12], and other acrylate-based polymers. ORMOCER and acrylate based resists are negative tone and polymerize via free-radical polymerization [7], [11]. For such resists, radicals generated from the exposure reactions initiate a polymerization reaction [13]. These polymerization-inducing radicals react with monomer molecules thereby activating them for further polymerization reactions. The activated monomer species react with other monomer species leading to a growing polymer chain. Competing reactions with polymerization propagation include neutralization by quenchers and termination of the polymer chains by reacting with each other.

The radical chain polymer reaction in LDWL could be represented by the following reaction equations [10], [13]–[15]:

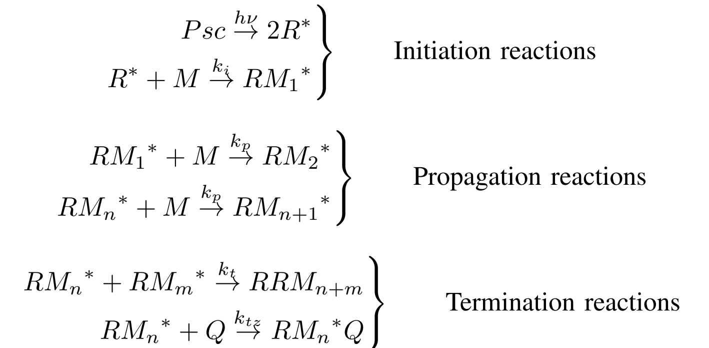

Where R^* represents the photoradicals; M represents the unactivated monomers; Q represents the quenchers; ${RM_n}^*$, for

TABLE II: Exposure parameters used in simulation

Parameter	*Value*	*Units*	*Ref.*
quantum yield (φ)	0.99×10^{-2}	no unit	fit
TPA cross-section (δ_{TPA})	1.0×10^{-48}	$cm^4.s.photon^{-1}$	[7]
SPA cross-section (δ_{SPA})	2.0×10^{-16}	cm^2	[7]
thermal conductivity (κ)	1.42×10^{-3}	$Wcm^{-1}K^{-1}$	[10]
monomer heat capacity (c_p)	1.89	$JK^{-1}g^{-1}$	[10]
monomer density (ρ)	1.07	gcm^{-3}	[10]
monomer concentration ($[M]$)	3.3×10^{-3}	$molcm^{-3}$	[10]
Psc concentration ($[Psc]$)	1.32×10^{-4}	$molcm^{-3}$	[10]
quencher concentration ($[Q]$)	2.88×10^{-8}	$molcm^{-3}$	[10]
monomer molar mass	200	$gmol^{-1}$	[10]
initial temperature (T_0)	293	K	choice
molar absorption (α)	373.83	cm^2mol^{-1}	[10]

$n \geq 1$, represents the activated monomers or growing polymer chain. The propagation reaction rate constants k_p is assumed to be the same for all $RM_n{}^*$. k_{tz} is the rate of termination by quenching reactions. Termination by the reaction of two activated monomers is k_t. In addition to these reactions, the monomers, quenchers and radicals can diffuse within the resist volume.

We model the polymerization reaction using the non-local diffusion driven polymerization model [16]. The corresponding equations were solved using a finite difference time domain method.

D. Development

Development involves the interaction of the resist with a developer. Most developers are made up of alkaline solvents: 2-propanol [1], isopropanol [11], cyclohexanone and methanol [17]. The inhibitor for radical polymerized resist systems is given by the polymer concentration. Several models have been developed for photoresists used in optical projection lithography systems, mask aligners and interference lithography [18]. We applied the original Mack model in the computation of the local development rates:

$$r = r_{max} \frac{(a+1)(1-m)^n}{a+(1-m)^n} + r_{min} \tag{3}$$

Representing a as another parameter m_{th}:

$$a = \frac{(n+1)}{(n-1)}(1-m_{th})^n \tag{4}$$

r_{max} is the development rate function for the unexposed regions of the resist. While r_{min} is the development rate function for the fully exposed regions of the resist. m_{th} is a measure of the relative polymer concentration needed for the structure to be developed. n defines the degree of selectivity of the developer; the higher the value of n, the more the developer behaves like a threshold filter between exposed and unexposed regions.

To compute the fabricated structure after development, the development rates from the Mack model [18] were supplied as inputs to a Fast Marching Algorithm [19]. This algorithm calculates the local developer arrival time at every position in the resist. It then propagates the development front (boundary between developer and resist) with a speed proportional to the local development rates. Spatial positions with arrival times less than the development time are washed away after development. The part of the resist that remains after this stage forms the fabricated profile.

TABLE III: Range of Mack parameters used in simulation

Parameter	*Value*
r_{max} (nm/s)	100.0
r_{min} (nm/s)	0.01
m_{th} (no units)	0.5
n (no units)	20

III. Model Application

A. Isolated voxel

We applied the model for the computation of feature sizes versus laser power and writing speed. The exposure time is defined as $0.1\mu m$ divided by the writing speed while the dark time was fixed at $0.5ms$. Using the obtained simulation results, we computed the upper and lower limits of the laser power needed to obtain single spot feature sizes within 5 percent, 10 percent and 15 percent tolerance of the target CDs.

Figure 2 (left) shows the change in transverse CD for laser powers in the range of $1-10mW$ and writing speeds from $5.0-10.0mm/s$. For increasing laser powers, across the range of simulated writing speed, the transverse CD increases at a reducing rate. The minimum laser power needed for polymerization to occur increases as the writing speed increases. This is due to shorter exposure durations at faster write speeds. These results closely match experimental literature results (Sun et al. 2002). Figure 2 (right) shows the laser power latitude (max-min power divided by mean laser power) versus the target CD. The minimum laser power is the laser power needed to fabricate the target CD minus the CD tolerance, while the maximum laser power is the power needed to fabricate the target CD plus the CD tolerance. The result on Figure 2 shows that printing smaller CDs implies a lower tolerance in laser power.

B. 3D patterns

We applied the simulation method to analyze the axial resolution of simple three-dimensional patterns. Specifically, a pair of mesas separated from each other along the axial direction and a woodpile like structure were simulated. The separation along the axial (z) direction at which the two structures, after fabrication, just do not touch each other specifies the axial resolution of the structure. The simulation result (Figure 3) shows that the axial resolution of the woodpile $(2.2\mu m)$ is better than that of the mesa array $(2.5\mu m)$. It is important to note that the patterns in Figure 3 only serve as axial resolution tests. In practice, structures have to be connected to the substrate after development; otherwise, the structures would fall apart.

IV. Conclusion

This paper presents a simulation approach for laser direct write lithography and demonstrated its application for the simulation of feature size versus laser power and writing speeds. We investigated the axial resolution of mesa-arrays and woodpile structures. The simulation flow can be used to optimize a LDWL fabrication process.

Acknowledgment

The first author gratefully acknowledges funding of the Erlangen Graduate School in Advanced Optical Technologies (SAOT) by the German Research Foundation (DFG) in the framework of the excellence initiative.

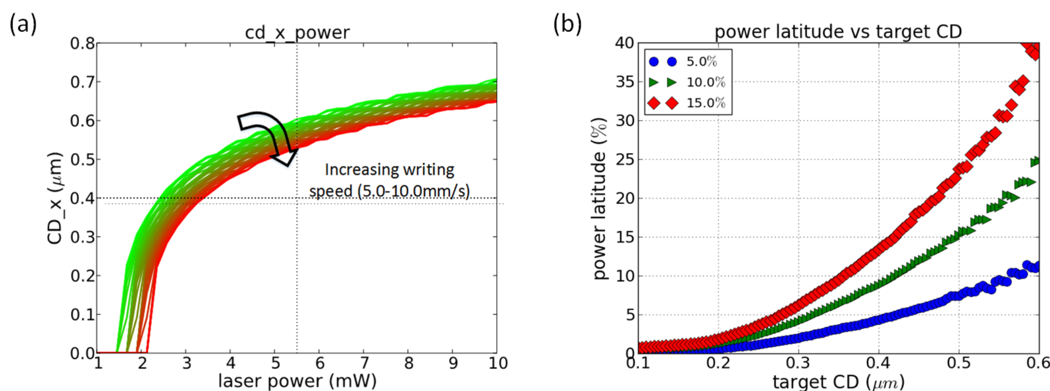

Fig. 2: (a) CD variation with laser power and writing speed. (b) laser power latitude needed to fabricate a specified feature versus the target CD for CD tolerances of 5%, 10%, 15%. Results obtained for two-photon absorption at NA = 1.0.

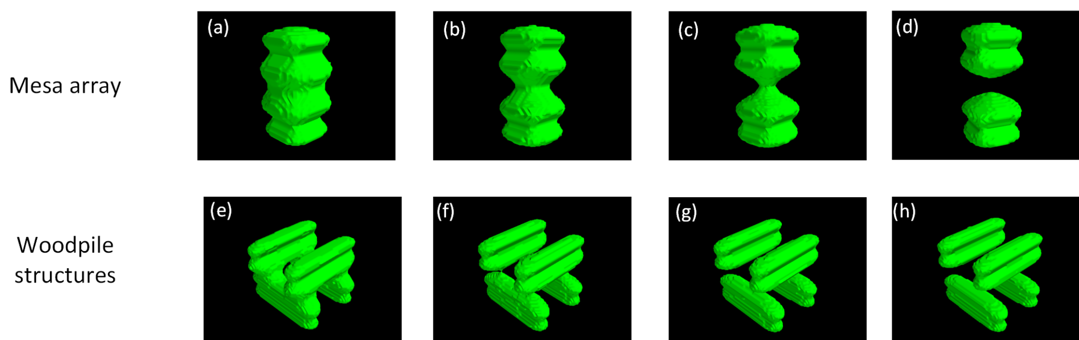

Fig. 3: (a,b,c,d) Mesas separated at distance $2.0, 2.2, 2.4, 2.5\mu ms$ respectively. (e,f,g,h) woodpile structures with axial separation of $2.0, 2.2, 2.4, 2.5\mu ms$ respectively. At $2.2\mu m$, the mesas are still joined to each other while the wood-pile structures are separated. Results obtained for two-photon absorption at NA = 1.4.

References

[1] J. Fischer, J. B. Mueller, J. Kaschke, T. J. A. Wolf, A.-N. Unterreiner, and M. Wegener, “Three-dimensional multi-photon direct laser writing with variable repetition rate,” *Optics express*, vol. 21, no. 22, pp. 26 244–26 260, 2013.

[2] J. B. Mueller, J. Fischer, Y. J. Mange, T. Nann, and M. Wegener, “In-situ local temperature measurement during three-dimensional direct laser writing,” *Applied Physics Letters*, vol. 103, no. 12, p. 123107, 2013.

[3] J. B. Mueller, J. Fischer, F. Mayer, M. Kadic, and M. Wegener, “Polymerization kinetics in three-dimensional direct laser writing,” *Advanced materials (Deerfield Beach, Fla.)*, vol. 26, no. 38, pp. 6566–6571, 2014.

[4] Fraunhofer IISB, “Dr. litho: Lithography simulation,” 2011. [Online]. Available: http://www.drlitho.com/html/pages/en_research_index.html

[5] M. Leutenegger, R. Rao, R. A. Leitgeb, and T. Lasser, “Fast focus field calculations,” *Optics Express*, vol. 14, no. 23, p. 11277, 2006.

[6] P. Evanschitzky, F. Shao, A. Erdmann, and D. Reibold, “Simulation of larger mask areas using the waveguide method with fast decomposition technique,” in *27th Annual BACUS Symposium on Photomask Technology*, ser. SPIE Proceedings, R. J. Naber and H. Kawahira, Eds. SPIE, 2007, p. 67301P.

[7] S. Engelhardt, “Direct laser writing,” in *Laser Technology in Biomimetics*, ser. Biological and Medical Physics, Biomedical Engineering, V. Schmidt and M. R. Belegratis, Eds. Berlin, Heidelberg: Springer Berlin Heidelberg, 2013, pp. 13–65.

[8] C. Decker and K. Moussa, “Real-time kinetic study of laser-induced polymerization,” *Macromolecules*, vol. 22, no. 12, pp. 4455–4462, 1989.

[9] Gustavo de Miguel, Martí Duocastella, Giuseppe Vicidomini, and Alberto Diaspro, “l/20 axial control in 2.5d polymerized structures fabricated with dlw lithography,” *Opt. Express*, vol. 23, no. 19, pp. 24 850–24 858, 2015.

[10] N. Uppal, “Modeling of temperature-dependent diffusion and polymerization kinetics and their effects on two-photon polymerization dynamics,” *Journal of Micro/Nanolithography, MEMS, and MOEMS*, vol. 7, no. 4, p. 43002, 2008.

[11] M. Malinauskas, M. Farsari, A. Piskarskas, and S. Juodkazis, “Ultrafast laser nanostructuring of photopolymers: A decade of advances,” *Physics Reports*, vol. 533, no. 1, pp. 1–31, 2013.

[12] R. Martinez-Duarte and M. Madou, “Su-8 photolithography and its impact on microfluidics,” in *Microfluidics and Nanofluidics Handbook*, S. Mitra and S. Chakraborty, Eds. CRC Press, 2011, pp. 231–268.

[13] G. Odian, “Principles of polymerization.”

[14] H. Li, Y. Qi, R. Malallah, and J. T. Sheridan, “Modeling the nonlinear photoabsorptive behavior during self-written waveguide formation in a photopolymer,” *Journal of the Optical Society of America B*, vol. 32, no. 5, p. 912, 2015.

[15] J. Qin, W. Guo, and Z. Zhang, “Modeling of the bulk free radical polymerization up to high conversion—three stage polymerization model. ii. number-average molecular weight and apparent initiator efficiency,” *Polymer*, vol. 43, no. 18, pp. 4859–4867, 2002.

[16] M. R. Gleeson and J. T. Sheridan, “Nonlocal photopolymerization kinetics including multiple termination mechanisms and dark reactions part i modeling,” *Journal of the Optical Society of America B*, vol. 26, no. 9, p. 1736, 2009.

[17] D. L. Forman, M. C. Cole, and R. R. McLeod, “Radical diffusion limits to photoinhibited superresolution lithography,” *Physical chemistry chemical physics : PCCP*, vol. 15, no. 36, pp. 14 862–14 867, 2013.

[18] C. Mack, *Fundamental Principles of Optical Lithography: Photoresist Development*, 1st ed. John Wiley and Sons, 2007.

[19] J. A. Sethian, “A fast marching level set method for monotonically advancing fronts,” *Proceedings of the National Academy of Sciences*, vol. 93, no. 4, pp. 1591–1595, 1996.